

# Experimental Study on Position Evolution and Load Transfer Law of Support in Large Dip Angle Stope Based on Digital Twin

Panshi Xie

Yan Chen

Shaogang Wu

Yang Hang

Key Laboratory of Western Mine Mining and Disaster Prevention, Ministry of Education, Xi 'an University of Science and Technology, Xi 'an, China; School of Energy, Xi 'an University of Science and Technology, Xi 'an, China

## ABSTRACT

In order to realize the intelligent mining of coal seam with large dip Angle, this paper adopts the methods of large proportion variable Angle loading threedimensional physical simulation experiment, numerical simulation and field measurement with digital twin technology. The hydraulic support with large dip Angle and large mining height is used as the prototype to design the physical entity model of 1:5 hydraulic support, combined with modeling and graphics rendering technology. Angle, displacement and load sensors were selected and placed to realize the data channel between the lower machine and the upper computer of the digital twin system, so that the position and load data of the physical entity model and the twin model of the laboratory hydraulic support could be shared in real time. Moreover, the multi-dimensional dynamic and static load transfer law and the position evolution characteristics of the support and surrounding rock under different inclination angles were analyzed. The results show that: with the

increase of the Angle of the working face, first, the initial support force required by the support decreases, and the damage degree of the roof increases; When the roof is soft, the lifting operation can avoid the instability of the support to a certain extent. Second, under the action of positive pressure, the load of the top beam under different angles is balanced; Under the backpushing action, the load in the upper inclined area of the shield beam increases gradually, while the load in the lower inclined area decreases gradually. Under the lateral push, the load changes periodically, and the load in each cycle is increased compared with that in the previous cycle. Third, the numerical simulation analysis shows that the load on the lower bracket is less than that on the upper bracket, and the load on the bottom of all the columns is greater than that on the middle and upper brackets. In order to reduce the impact of the columns on the bottom plate or the base, it is necessary to improve the anti-subsidence ability of the base. Finally, according to the research results, the improvement and optimization measures of the support are put forward, and the field test shows that these measures effectively solve the problems of sinking, sliding and tipping of the support in the working face with large inclination Angle, and obtain good application results.

---

Supported by the National Natural Science Foundation of China (Grant No.52174126 and 52104147), Shaanxi Outstanding Youth Science Foundation Project (2023-JC-JQ-42), Shaanxi University Youth Innovation Team Project

## INTRODUCTION

High inclination coal seam refers to the coal seam with a burial inclination of  $35^{\circ} - 55^{\circ}$ , which is recognized as a difficult coal seam in the domestic and foreign mining circles [1-4]. As we all know, hydraulic support is the most important supporting equipment of working face. In the mining process of longwall working face of high inclination coal seam, the change of spatial position and multi-dimensional load transfer law of the support are more complicated, so it is of great theoretical and practical significance to realize intelligent mining of this kind of coal seam.

In the past 50 years, the mechanized mining of large-dip and steep-dip coal seams in China has experienced difficulties. It was not until 1998 that the longwall fully mechanized mining technology of large-dip medium-thick coal seam in Lushuidong Coal Mine of Huaying Mountain in Sichuan Province achieved success, making relevant research and practice in China at the forefront of this field, and on this basis, continuous exploration and practice have been carried out[5].

The University of Nottingham combined virtual reality and other computer science technologies to create rich mining virtual reality models in modeling software, thus achieving significant social benefits[6]. MARARCO established a virtual reality design and analysis system for mining engineering using real mine data to simulate the design, construction, mining and other links of mining engineering [7-8]. Hu Yanchao et al.

cal virtual intelligent workshop training system, which enables production personnel to master the application skills of mechanical manufacturing safely and efficiently [9]. Illinois State University used this technology to achieve multi-person remote collaborative design, thereby reducing development time[10-11].

Digital twin technology refers to the use of data to drive the virtual model in the virtual space to have the same behavior as the corresponding entity in the object space, so as to realize the observation, prediction and optimization of physical entities [12-16]. For the first time, NASA applied the concept of digital twins to the field of intelligent manufacturing, which is used to simulate and analyze the state of space vehicles during flight, so as to realize the prediction and monitoring of flight states.

Therefore, In the laboratory environment, this paper integrates digital twin technology to carry out physical similarity simulation experiment of hydraulic support with high inclination Angle[1718], realizing the perception of mechanical behavior of the support to surrounding rock and equipment, revealing the dynamic law of multidimensional load transfer of surrounding rock and equipment

to the support during the process of initial bracing, shifting and pushing under the inclination effect, as well as the temporal and spatial characteristics of mechanical response of the support and other equipment. It provides important theoretical support for the dynamic stability control of hydraulic support for long wall working face with high inclination Angle.

## DEVELOPMENT OF HYDRAULIC SUPPORT TWIN SYSTEM

### System Design Framework

Based on virtual simulation technology, the twin system of hydraulic support and the main platform of three-dimensional mechanical behavior experiment of layered mining coal and rock mass is designed, and a three-dimensional visualization operation and simulation platform is established to truly present the actual operating status of the hydraulic support model with large inclination Angle, which can realize monitoring, remote operation and virtual operation, and analyze and process the results, as shown in Figure 1.

This system consists of four major modules:

#### 1. User module

The user module realizes the login function of administrator and common user. Ordinary users can only view their own experimental data, the administrator has the permission to view all experimental data, and can set accounts for ordinary users.

#### 2. Sensor module

The sensor module consists of two parts: data acquisition and data upload. Data acquisition is to collect motion state data of inclination sensor, displacement sensor and oil pressure sensor; The data upload part refers to the processing of the data collected by the sensor to the network port.

#### 3. Data module

The data module is mainly responsible for data reception and data storage. Among them, the data receiving module refers to the process of the host computer ( this system refers to the industrial computer installed with the twin map software system ) reading the data collected by the sensor through the port of the protocol to ensure that the data can be effectively received and processed by the system ; data storage refers to the process of storing all attitude data to the cloud database after the data is filtered and processed by the twin system, combined with the motion analysis of the hydraulic support in this paper.

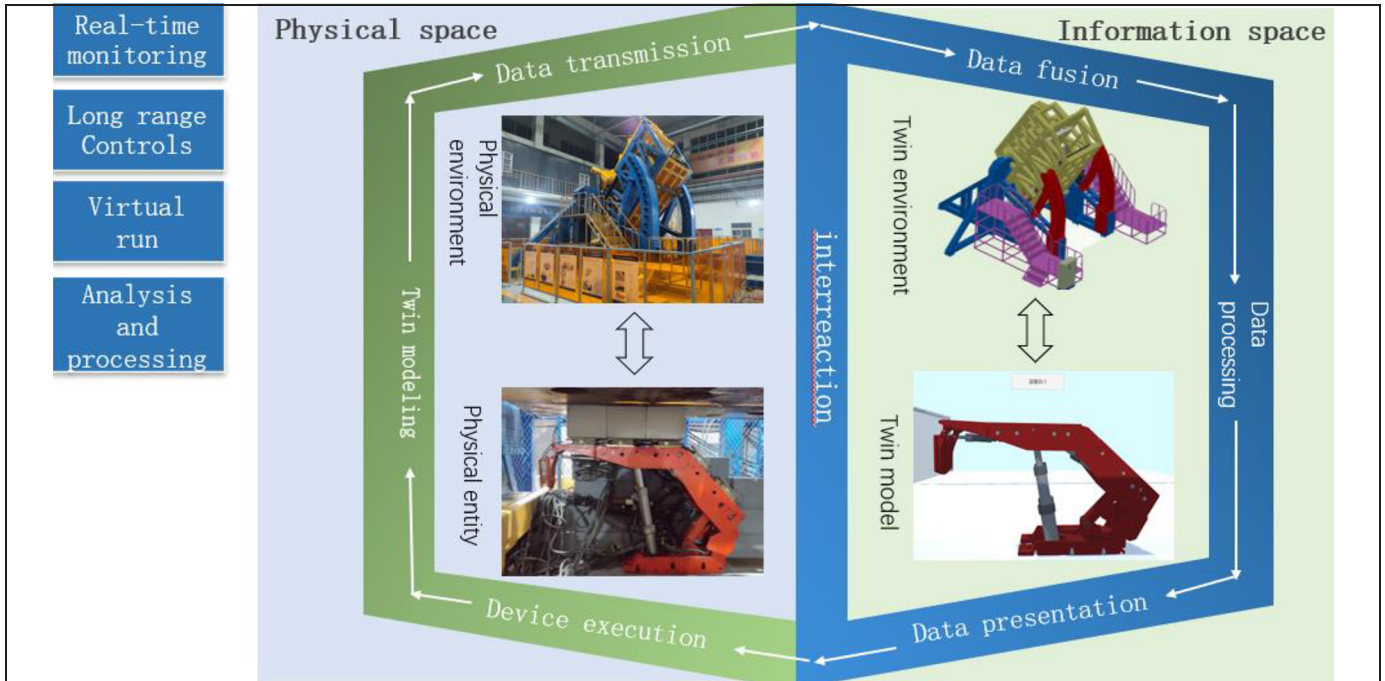


**Figure 1. Composition of attitude sensing and simulation system of hydraulic support**

#### 4. Data display module

Data display module includes data matching and data display functions. Data matching refers to matching the attitude data transmitted by the lower machine with each component of the hydraulic support, so as to facilitate subsequent display. The function of data display is to combine the matched data with the hydraulic support model through the program written, so that the model support and the solid support move synchronously, and at the same time, the load and inclination situation of the support is drawn in real time line chart, so that the experimenter can intuitively monitor the movement and load state of the hydraulic support, which is conducive to the analysis of the experimental data later. When there are special cases such as tipping, sliding, biting, etc. on the working face with large inclination Angle, users can be reminded to make corresponding control actions.

#### Physical Model Composition

In view of the major needs of safe and efficient green development and utilization of coal seams under complex burial conditions, a multifunctional variable Angle large-proportion “support surrounding rock” system physical simulation and simulation experimental platform was developed and manufactured, which was used to study and solve the basic scientific problems, key technical problems and field process problems of safe and efficient mining of complex and difficult coal seams.

The platform is composed of an outer frame and an inner frame, as shown in Figure 2. The inner frame Angle is adjustable from 0° to 67° without pole and has stage locking. Four groups of hydraulic systems are arranged to realize synchronous or asynchronous loading in vertical direction within the above inclination range. The platform is suitable for different burial conditions, and can simulate the physical environment of the working face with an inclination of 0°~67°, dynamically monitor the posture and state of the hydraulic support, realize the mining technology experiment of the stope, load loading and load control of the roof and floor, and carry out the dynamic simulation of the spatial interaction between the support and surrounding rock with a large scale support model (1:5).

The platform can realize the dynamic and static controllable loading of coal rock mass or support in the frame of the model. Load control PLC system is built in the test bench, and a force closed loop composed of proportional servo valve and pressure sensor is arranged to control the output of hydraulic cylinder. The loading requirements of coal and rock mass or support in the inner frame space can be achieved with a maximum loading pressure of 0.2 MPa, which can be realized either by setting the value of each loading point individually (combined) or by periodic pressure simulation loading, or by impact pressure simulation loading. The specific parameters of the test bench are shown in Table 1.

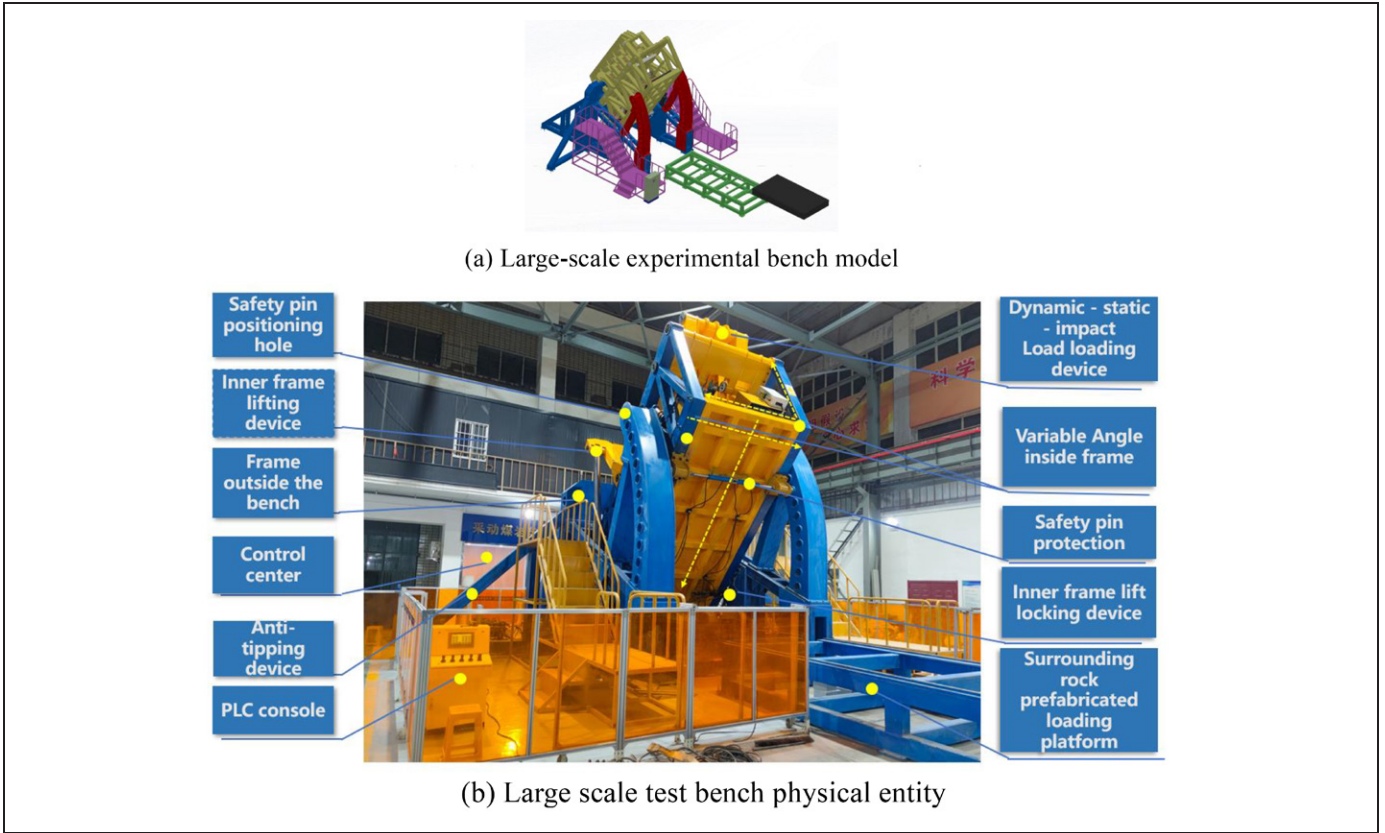


Figure 2. Large scale experimental bench

Table 1. Experimental platform parameters

Item	Parameter Description
Outer frame length, width and height	11 m×8.5 m×7.5 m
Inner frame length, width and height	4.2 m×2.4 m×1.7 m
Inner frame inclination range	0–67° stepless adjustable
Load hydraulic cylinder stroke	200 mm
Vertical and lateral loading pressures	0–0.2 MPa
Load pressure sensor range	35 t

The physical model of hydraulic support is based on the support of a mining machine manufacturer and is made according to the geometric similarity ratio 5:1. The model not only has the basic functions of the prototype support, but also has the functions of pressure relief, side protection, side adjustment and bottom lifting. The hydraulic support completed in design is shown in Figure 3, the similarity ratio of bulk density  $\alpha_\gamma = \gamma_p/\gamma_m = 1$ , the similarity ratio of strength  $\alpha_\sigma = \sigma_p/\sigma_m = \alpha_l \cdot \alpha_\gamma = 5$  and similarity ratio of external force  $\alpha_F = \alpha_\sigma \cdot \sigma_l^2 = 125$ , and the specific parameters are shown in Table 2.

Table 2 Parameters of hydraulic support

Parameter Name	Solid Support Parameter	Model Support Parameter
Height of support	2,200–4,500 mm	440–900 mm
Rated working resistance	7000 kN	56 kN
Rated initial holding force	5,066 kN	40.528 kN
Support width	1,680–1,880 mm	336–376 mm
Adapt to the inclination of the working face	$\leq 60^\circ$	$\leq 67^\circ$
Pumping station pressure	31.5 MPa	6.3 MPa

### Attitude Analysis of Hydraulic Support Physical Model

The hydraulic support is mainly composed of a base, a column, a top beam, a cover beam, a protection plate, a hydraulic cylinder, a support rod, a traction rod and other components, which work together to achieve the lifting and moving functions of the support. In the process of movement, each component does not move as an individual, but cooperatively, so it is necessary to measure and calculate the spatial configuration of each component at each time point.

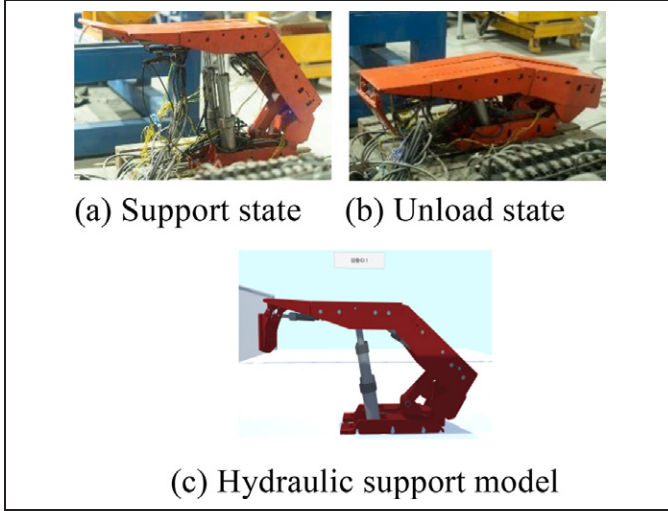


Figure 3. Hydraulic support model

In the movement of the hydraulic support, the hydraulic cylinder plays a key role. Through the liquid pressure in the hydraulic cylinder, the hydraulic cylinder rod extends or retracts outwards, thus driving the lifting of the support body. The hydraulic support diagram is shown in Figure 4. In the lifting motion, the base is fixed, and the hydraulic support extends out of the first column to the highest position, and then extends out of the second column to the highest position. In this process, the lifting height of the top beam is relative to the height  $l_3$  of the base, as shown in equation (1):

$$l_3 = L_1 \sin \theta_1 + L_2 \sin \theta_2 \quad (1)$$

where,

- $L_1$  = the length of the cover beam are fixed
- $\theta_2$  = the Angle between the shield beam and the plane where the base is located can be obtained by reading the inclination sensor
- $L_2$  = the rear connecting rod in the four-link structure has a fixed length
- $\theta_1$  = The Angle between the rear connecting rod and the base plane can be obtained by reading the inclination sensor.

The length of the secondary column is shown in Formula (2): (Because the primary column takes the base column as the parent object, the available length indicates the real-time status of the support, the same below)

$$l_5 = l_3 \sin \theta_3 - l_8 - l_4 \quad (2)$$

$l_4$ , the height of the first level column is shown in Formula (3):

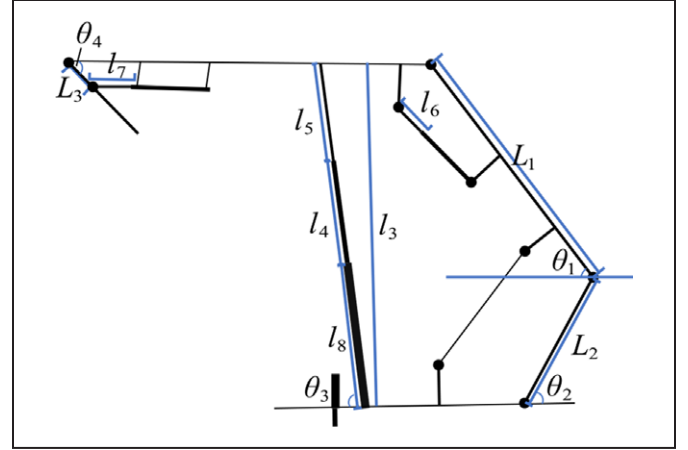


Figure 4. hydraulic support profile diagram

$$l_4 = l_3 \sin \theta_3 - l_8 \quad (3)$$

In the working process of hydraulic support, the protection plate is a very important part, and its motion state directly affects the stability of the coal wall and the safety of the shearer driver. In the working process, the protection plate is controlled by the hydraulic cylinder. Specifically, the piston rod of the hydraulic cylinder is connected with the guard plate, and the hydraulic oil of the hydraulic cylinder controls the expansion and expansion of the piston rod, so as to realize the rotation of the guard plate around the top beam and the hinge of the guard plate. The angle of the guard plate can be obtained by installing an inclination sensor, and the extension of the piston rod connected with the guard plate  $l_7$  is shown in Formula (4) :

$$l_7 = \begin{cases} L_3 \cos \theta_4 & (\theta < \frac{\pi}{2}) \\ L_3 \sin \theta_4 & (\theta \geq \frac{\pi}{2}) \end{cases} \quad (4)$$

where,

- $L_3$  = the distance between the upper side plate and the top beam and the upper side plate and the piston rod is a fixed value;
- $\theta_4$  = Angle between the beam and the guard plate can be obtained by reading the sensor.

### Collection of Attitude and Load Information of Hydraulic Support Model

#### Attitude Information Acquisition of Hydraulic Support

In the digital twin system, it is often necessary to collect the position and attitude information of physical objects through sensors, and reflect it in real time in the digital twin system, so as to achieve the purpose of accurately simulating the real world.

The MPU6050 six-axis attitude sensor, which integrates the three-axis accelerometer and the three-axis gyroscope, can provide the attitude information of six degrees of freedom at the same time, and effectively reduce the cumulative error of the gyroscope when it is stationary and the motion error of the accelerometer when it is moving, so as to improve the measurement accuracy and stability.

According to the above formula (1)–(4), the collection position is shown in Figure 5.

The VL53L0X laser ranging sensor with second-generation FlightSense™ technology, developed by ST, is used for displacement acquisition to achieve high precision, low power consumption and strong anti-interference absolute distance measurement, and is independent of target size, color and reflectivity, effectively reducing ambient light interference. The collection position is shown in Figure 6.

### Hydraulic Support Load Information Acquisition

Oil pressure sensor is a kind of fluid pressure sensor, which is mainly composed of sensor body, measuring diaphragm, conductive diaphragm, sensitive element and signal processor. It usually has the characteristics of high precision, high reliability, fast reaction speed, etc., and can be widely used in pressure control, safety protection, machine and equipment control of hydraulic systems. The collection position is shown in Figure 7.

The hydraulic cylinder oil pressure is used to determine the load at different positions. The relationship between the load  $q$  and the oil pressure  $P_0$  is as follows:

$$q = \frac{P_0}{S} \quad (5)$$

$S$  is the area of specific parts of the hydraulic.

### Twin Modeling Based on Unity3D

Twin system design needs to model the hydraulic support, open SolidWorks to create a new part file, create features combined with the motion attitude analysis of the hydraulic support, and assemble in a “topdown” way. Because the model built by SolidWorks will lose the structural relationship when opened in Unity 3D, Therefore, it is necessary to import the model into Maya for model rendering, and then export the.fbx format file of Maya into Unity3D, which is usually written in C# or UnityScript. Unity3D will automatically read and display the preview of the model in the scene.

### Function Realization

Click the large Angle hydraulic support twin system to enter the login page, you can choose ordinary user login and administrator login. Test a complete motion state of

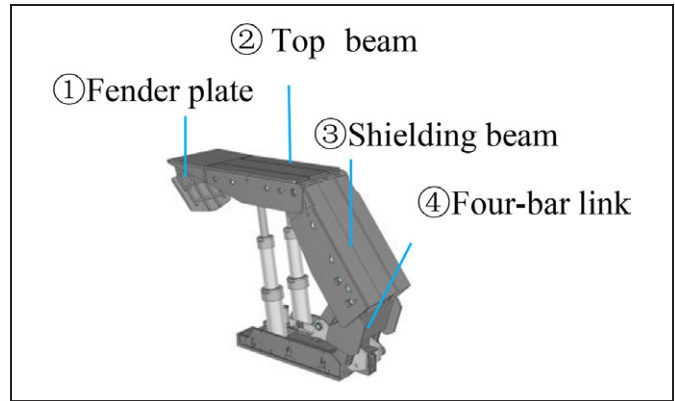


Figure 5. Schematic diagram of Angle acquisition position

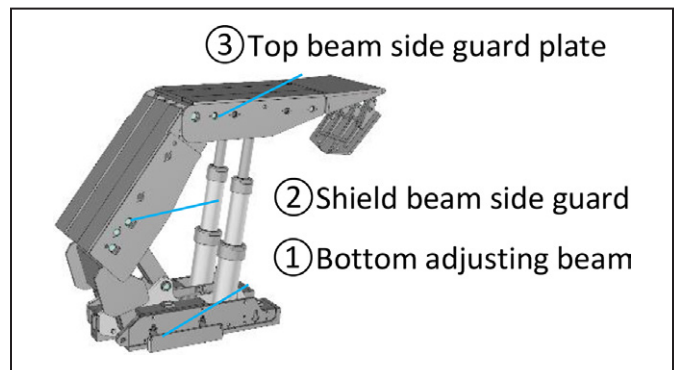


Figure 6. Schematic diagram of displacement acquisition position

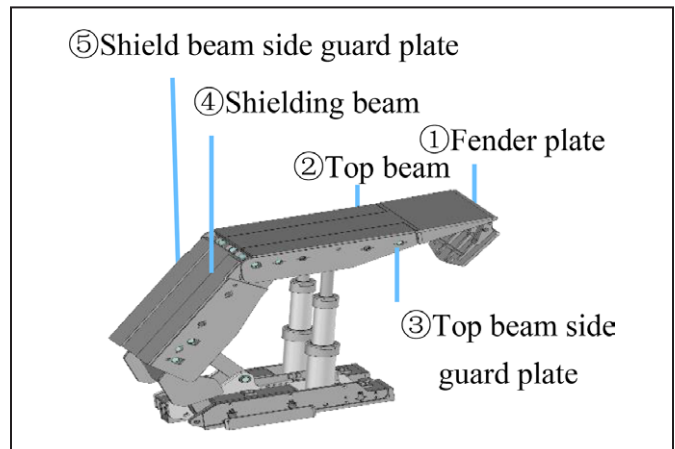


Figure 7. Schematic diagram of oil pressure collection position

the hydraulic support, including the lifting frame, lifting the protection plate, extending the side push jack, extending the bottom push rod, folding the bottom push rod, folding the side push jack, folding the protection plate, and lowering the frame. The individual modules of the twin system are examined in this complete state.

As shown in Figure 8, Figure (a) (b) (c) is the real model when the support is raised, and the twin models of figure (d) (e) (f) can move synchronously with the real support.

## PHYSICAL SIMILARITY SIMULATI EXPERIMENT

### Project Overview

A working face of a mine is located in the No. 5 coal seam of the second mining area. The surface of the working face is high and gully, with a narrow distribution in the east and west, and low in the west. The design strike length of the working face is 2098 m and the dip length is 105 m. The coal seam inclination of the working face is 36°–46°, with an average of 44°. The occurrence of coal and rock is stable. The coal and rock characteristics of the working face are shown in Table 3.

The working face adopts comprehensive mechanized large mining height mining technology, mining height of 3.5–4.2 m. The process flow of downward cutting coal → upward clearing floating coal → moving frame → pushing conveyor is adopted. According to the technical conditions of mine production, 60 ZZ7000/22/45 two-column hydraulic support and 3 ZZG2000/22/45 transition supports were selected for the working face.

### Experimental Method

Some scholars classify the dynamic load on the large-angle bracket as compressive dynamic load and inter-frame (side push) dynamic load. The dynamic load can be divided into positive pressure impact and push back impact according to the dynamic load position. This type of dynamic load has great harm, especially in the environment of stope with

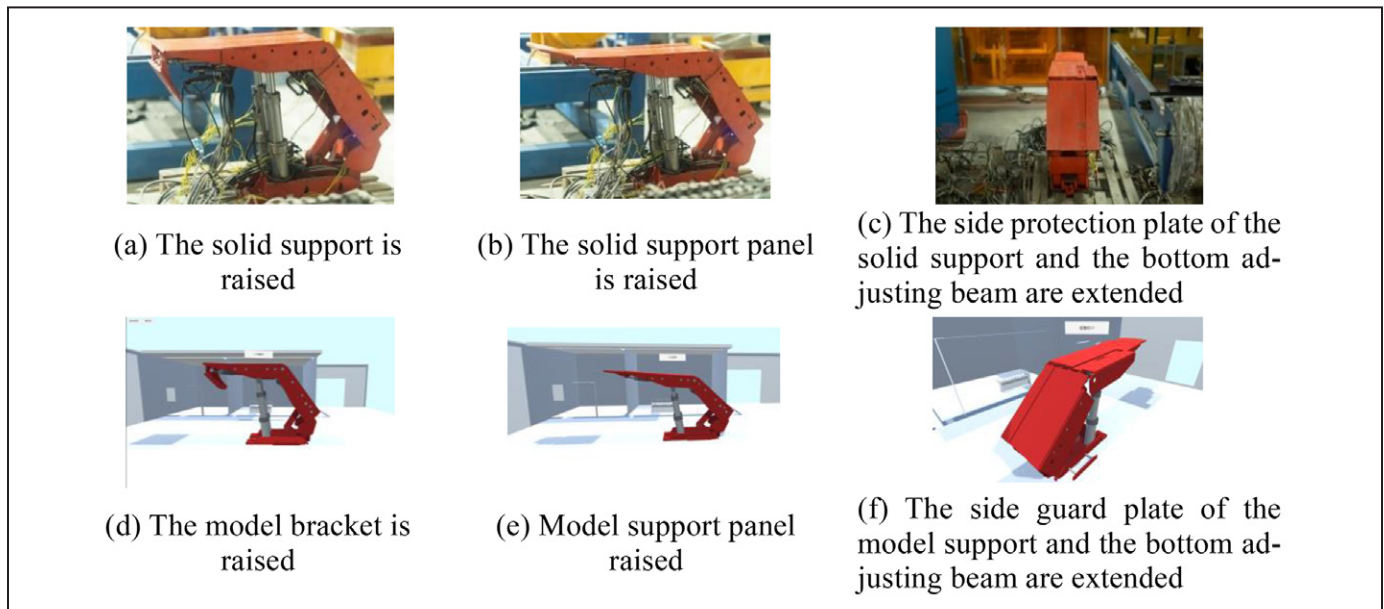


Figure 8. 1:1 mapping of solid model hydraulic support

Table 3. Physical and mechanical characteristics of coal and rock at working face

Name	Name of Coal and Rock	Thickness, m	Compressive strength, MPa	Peculiarity
Basic roof	Medium sandstone	16.59	100.2	Mainly quartz, strong resistance to weathering, layer development
Direct roof	Pebbly coarse sandstone	2.32	79.9-100.2	Grayish white, argillaceous cement, weathering fragile
Coal seam	5# Coal	3.58-9.77	3-5	Contains 3-5 layers of dirt, coal dirt interlayer 1.4-2.5 m
Direct bottom	Carbonaceous mudstone	17.06	9.14-12.76	Grayish white, mineral cement
Basic bottom	gritstone	9.0	78	Joint development, weathering brittle

large inclination Angle and large mining height, it will cause the phenomenon of support crushing and sometimes even affect the stability of return air roadway. The dynamic load between frames is caused by the tipping or sliding of the upper bracket under the impact along the tilt, causing the dynamic load between the frames on the lower bracket.

The dynamic and static loads as shown in equation (6) are applied to 35°, 45°, 55° and 65° inclination angles respectively on a large scale experimental bench. The dynamic load can be divided into three types: positive pressure impact, backward thrust impact and lateral thrust impact. The static load  $P_0$  is 40 kN, and the load increase amplitude  $P_r$  is 0 kN; Under dynamic load, positive pressure impact  $P_0$  takes 40 kN and  $P_r$  takes 8 kN; Lateral thrust impact  $P_0$  is 5 kN,  $P_r$  is 0.8 kN; Push-back impact  $P_0$  takes 3 kN and  $P_r$  takes 0.48 kN.

$$P(t) = P_0 + P_r e^{-30.0t} \sin(60.0t) \quad (6)$$

The twin system can be used to monitor the position status and load information of the hydraulic support (referring to the value of the oil pressure sensor in the pumping station) in real time in the large screen of the multidimensional experimental platform for the dynamic behavior of layered coal and rock mining, as shown in Figure 9 (a). In addition, the Android client of the twin system has been developed, as shown in Figure 9 (b), to facilitate researchers to view the internal information of the experimental platform in real time around the experimental platform. At the same time, the system also uses high-definition surveillance cameras to monitor internal information when the experimenters cannot enter directly, as shown in Figure 9 (c).

As shown in Figure 10, a bridge crane is used to send the hydraulic support into the model preset device, and then

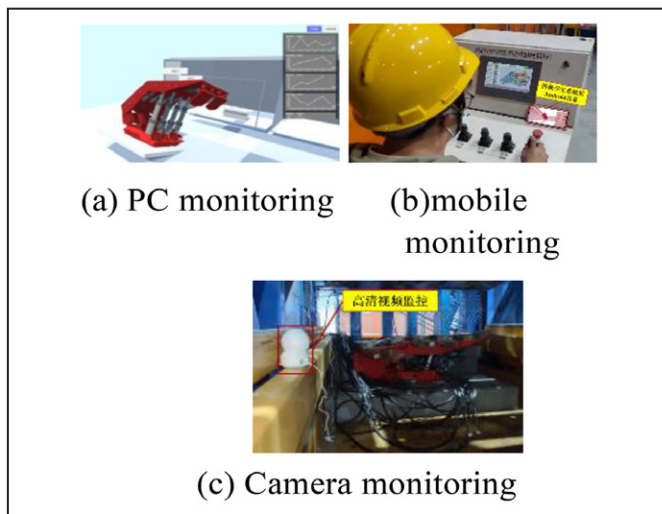


Figure 9. Experimental data monitoring

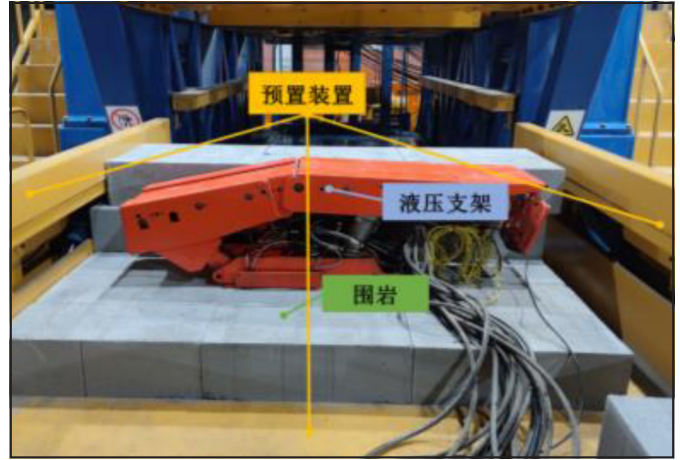


Figure 10. Experimental materials



Figure 11. Inside the experimental bench

a special material with compressive strength of 18 MPa is laid around the hydraulic support as the surrounding rock, and finally the hydraulic support and surrounding rock are sent into the experimental platform with the preset device. Inside the test stand, as shown in Figure 11, the sensor array is covered above the support, the false roof and coal wall are arranged, and the hydraulic support is raised to make the test stand fully contact with the system composed of “support and surrounding rock”, as shown in the figure, and then the loading experiment is carried out.

### Experimental Analysis

The Angle of the large scale test bench was adjusted to 35° to 65°, and static loads were applied to the roof and hydraulic support, as shown in Figures 12–15(a) the solid model under different inclination angles, and (b) the twin model under different inclination angles.

At 35° inclination Angle, when no load is applied to the hydraulic support, the average load of the sensor on the top

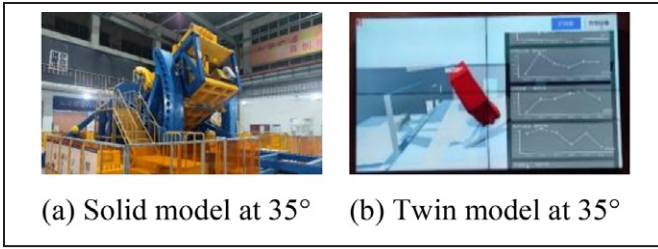


Figure 12. Inclination model of 35°

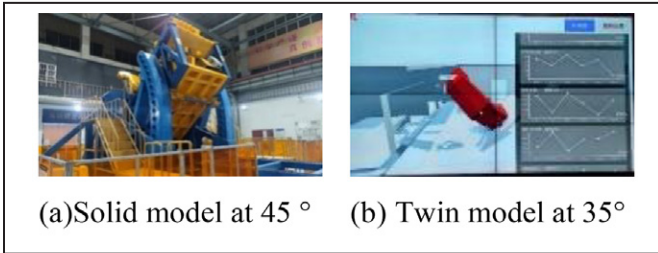


Figure 13. Inclination 45° model

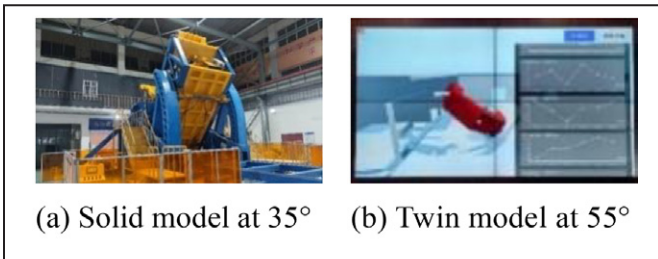


Figure 14. Inclination 55° model

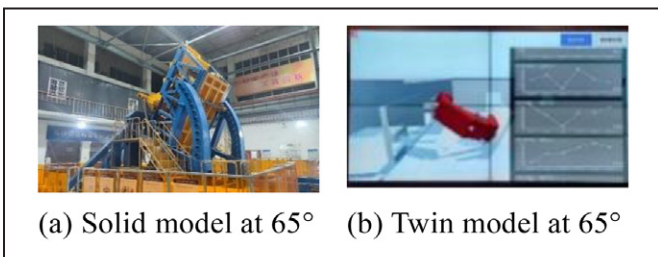


Figure 15. Inclination 65° model

beam of the support is 1.69 kN (corresponding to 0.86 MPa in the field), and the total load is 15 kN (7.65 MPa). During the loading process, the average load of the support sensor gradually increases to 4.1 kN (2.09 MPa), and the total load is up to 36.9 kN (18.83 MPa), and then the top beam drops to 0 kN instantly, as shown in Figure 16(a). High-definition monitoring shows that the top plate slides to the inclined lower support area after breaking. The twin system showed that the support tipped 3.4° in the tilt direction and then quickly returned to normal, increasing the average sensor load to 1.5 kN (0.77 MPa). This is because the

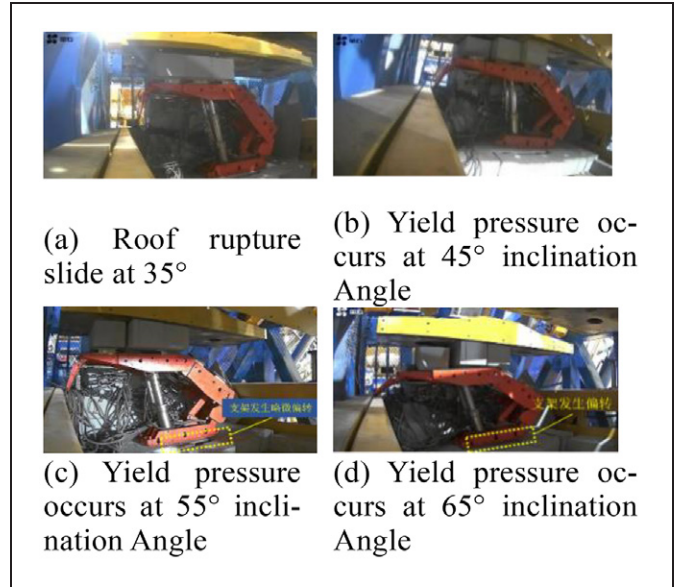


Figure 16. Changes of loading brackets at different angles

support adopts the constant pressure support mode, which can quickly carry out the lifting operation when the top plate (bottom plate) is broken, increase the working resistance, and avoid the instability of the support.

At 45° inclination Angle, when no load is applied to the hydraulic support, the average load of the sensor on the top beam of the support is 1.65 kN (0.84 MPa), and the total load is 14.85 kN (7.58 MPa). During the loading process, the average load of the support sensor gradually increased to 4.3 kN (2.19 MPa), the total load reached 38.7 kN (19.74 MPa), and then the total load of the top beam dropped to 35.1 kN (17.90 MPa). The twin system showed that the height yield of the hydraulic support column was 3.7 cm, as shown in Figure 16(b). When the total load reached 38 kN (19.39 MPa), the roof broke, the high-definition monitoring showed that the roof slipped to the support area below the tilt, the twin system showed that the support fell 4.2° in the tilt direction, and then quickly returned to normal, and the average sensor load increased to 1.7 kN (0.87 MPa).

At 55° inclination Angle, when no load is applied to the hydraulic support, the average load of the sensor on the top beam of the support is 1.39 kN (0.71 MPa), and the total load is 12.51 kN (6.38 MPa). During the loading process, the average load of the support sensor gradually increased to 4.4 kN (2.24 MPa), the total load reached 39.6 kN (20.20 MPa), and then the total load of the top beam dropped to 36.4 kN (18.57 MPa). The twin system showed that the height of the hydraulic support column yielded 6.7 cm, and the pressure continued. When the total load reached 36 kN (18.36 MPa), the roof broke, as

shown in Figure 16(c). High-definition monitoring showed that the roof slipped to the support area below the tilt, the twin system showed that the support fell 4.2° to the tilt direction, and the average load of the sensor increased to 1.64 kN (0.84 MPa) after the initial support was restored. At this time, the support base is slightly deflected, and there is a greater possibility of tipping instability.

At 65° inclination Angle, when no load is applied to the hydraulic support, the average load of the sensor on the top beam of the support is 1.21 kN (0.62 MPa), and the total load is 10.89 kN (5.56 MPa). During the loading process, the average load of the support sensor gradually increased to 4.3 kN (2.19 MPa), the total load reached 38.7 kN (19.74 MPa), and then the total load of the top beam dropped to 36.4 kN (18.57 MPa). The twin system showed that the height of the hydraulic support column yielded 13.6 cm, and the pressure continued. When the total load reached 38.7 kN (19.74 MPa), the roof broke, as shown in Figure 16(d). High-definition monitoring showed that the roof slipped to the support area under the tilt, and the twin system showed that the support fell 7.1° to the tilt direction, and the support did not recover the initial support.

During the twin system extraction experiment, the inclination of the hydraulic support along the inclined direction is shown in Figure 17, where the horizontal axis represents the time to start loading and the vertical axis represents the inclination magnitude. Under the conditions of 35° and 45° working face inclination Angle, the support becomes unstable after the roof is broken, because the support adopts the constant pressure support mode, and then the support has lifting operation, and the support returns to the original inclination Angle. Under the condition of 55° and 65° working Angle, after the instability of the support, the lifting operation can not restore the support to the original working state. It can be found in the figure that with the increase of working face inclination, the time of support instability appears earlier and earlier. The support from the beginning of instability (Angle begins to decrease) to the automatic adjustment of the balance (Angle begins to increase) time is increasingly longer, at 35° about 0.5s, at 65° about 0.8s. The Angle variation of the bracket also increases with the increase of the Angle. When the Angle varies from 35° to 65°, the Angle variation is 3.4°, 4.2°, 4.2° and 7.1°, respectively. With the increase of the Angle, it is more and more difficult for the bracket to recover to the original Angle after instability.

Under the four inclined angles, the broken state of the roof is different. As shown in Figure 18 (a), under the condition of 35°, the roof breaks under load, impacting the

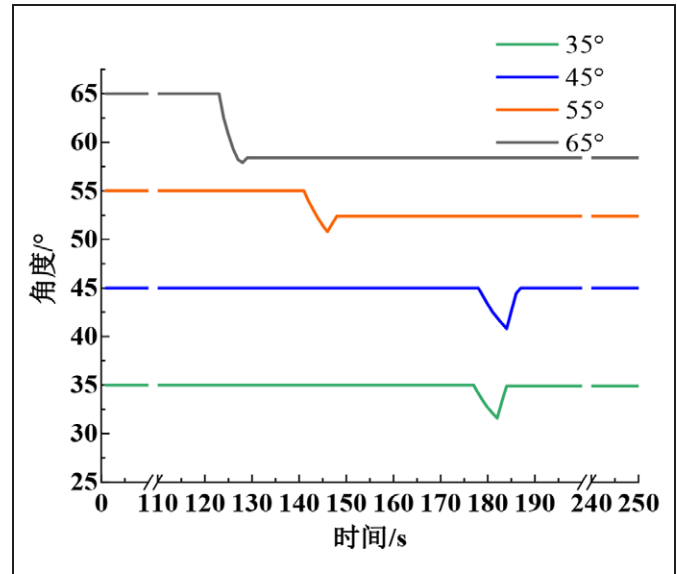


Figure 17. Changes of bracket Angle under different inclination angles

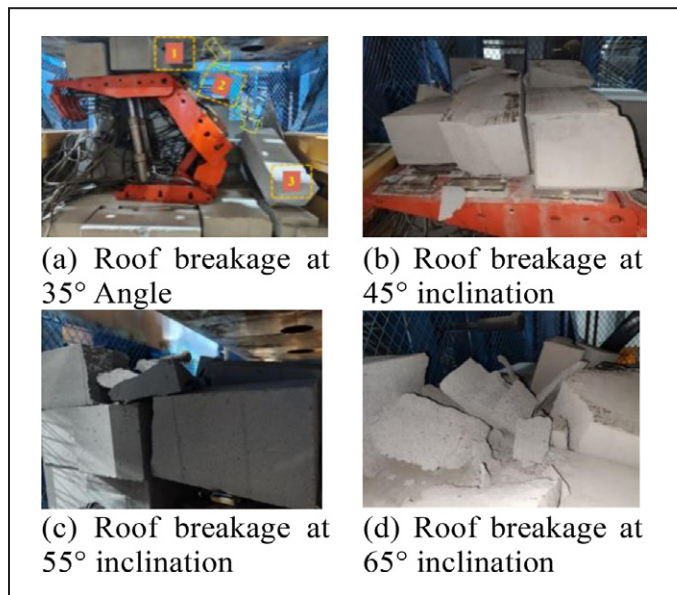


Figure 18. Broken state of roof under different

shield beam and then sliding to the goaf, resulting in a large broken rock mass of the roof. As shown in Figure 18 (b), under the condition of 45° inclination Angle, the fracture degree of the roof strata is greater than that of 35°, but there are still large rock strata at this time. As shown in Figure 18(c), when the inclination is 55°, the roof strata are seriously broken, and large rock strata are relatively rare. As shown in Figure 18 (d), when the inclination reaches 65°, it is difficult to see large broken rock layers and the roof is seriously broken. It shows that with the increase of inclination Angle, the degree of fracture of roof strata increases, and the

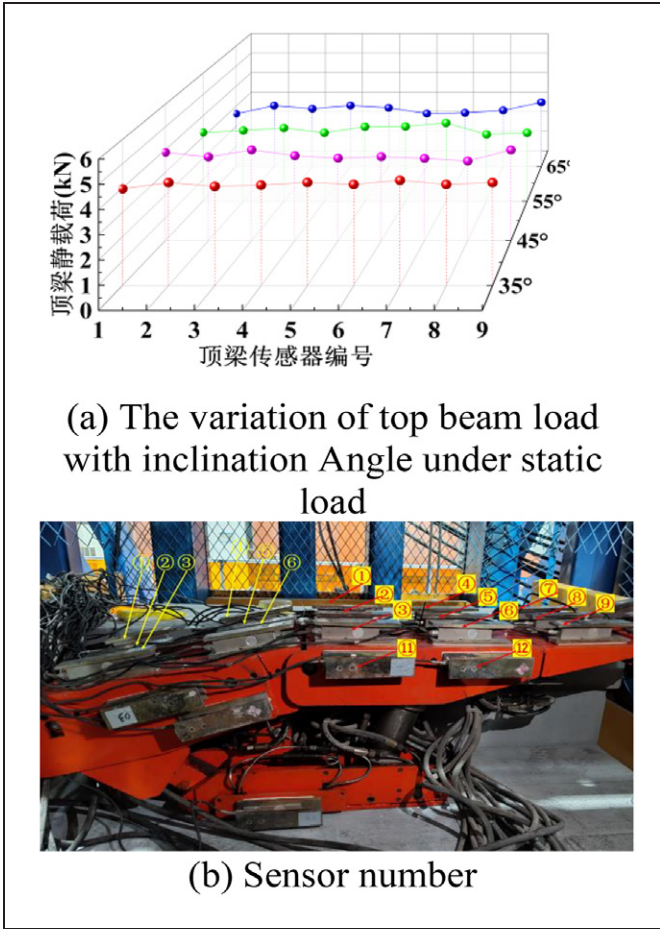


Figure 19. Variation of top beam load with tilt Angle under static load

“stent-surrounding rock” system is difficult to maintain the working resistance required by the support, and it is easier to topple and lose stability.

When the inclination Angle is 35°, 45°, 55° and 65°, as shown in Figure 19(a), the static load of 40 kN is applied to the top beam, and the average load of the top beam is 4.16 kN, 3.74 kN, 3.35 kN and 2.86 kN respectively. When the static load is applied to the top beam, with the increase of the inclination Angle, the average load gradually decreases. The component of gravity perpendicular to the rock layer gradually decreases. Sensor numbers are shown in Figure 19(b). Sensors No. 1, 2 and 3 (upper inclined area) > No. 4, 5 and 6 (middle inclined area) >

No. 7, 8 and 9 (lower inclined area) under four different inclination angles. The inducement of the above characteristics is mainly caused by the unbalanced load of the support under the Angle effect.

When the inclination angles are 35°, 45°, 55° and 65°, as shown in Figure 20(a), under the positive pressure impact, the average load of the top beam is 3.47 kN,

3.62 kN, 3.69 kN and 3.57 kN respectively, and there is no significant difference in the load under the four inclination angles, which is because the dynamic load impact has a short impact time and the load is relatively uniform under the positive pressure impact.

When the inclination angles are 35°, 45°, 55° and 65°, as shown in Figure 20 (b), the sensors on the shield beam show the characteristics that No. 5 and 6 sensors (upper inclined area) have the largest load, followed by No. 3 and 4 sensors (middle of the top beam), and No. 1 and 2 sensors (lower inclined position) have the smallest load. With the increase of inclination Angle, the load on the upper part of the shield beam gradually increases, while the load on the lower part decreases.

Under the lateral thrust impact, as shown in Figure 20(c), the load reading of the two sensors on the side of the top beam is significantly greater than that of the sensor on the surface of the top beam. The load reading of the surface sensor is said to change periodically, and the value of each period is greater than that of the previous period. As the inclination increases, all sensor readings increase.

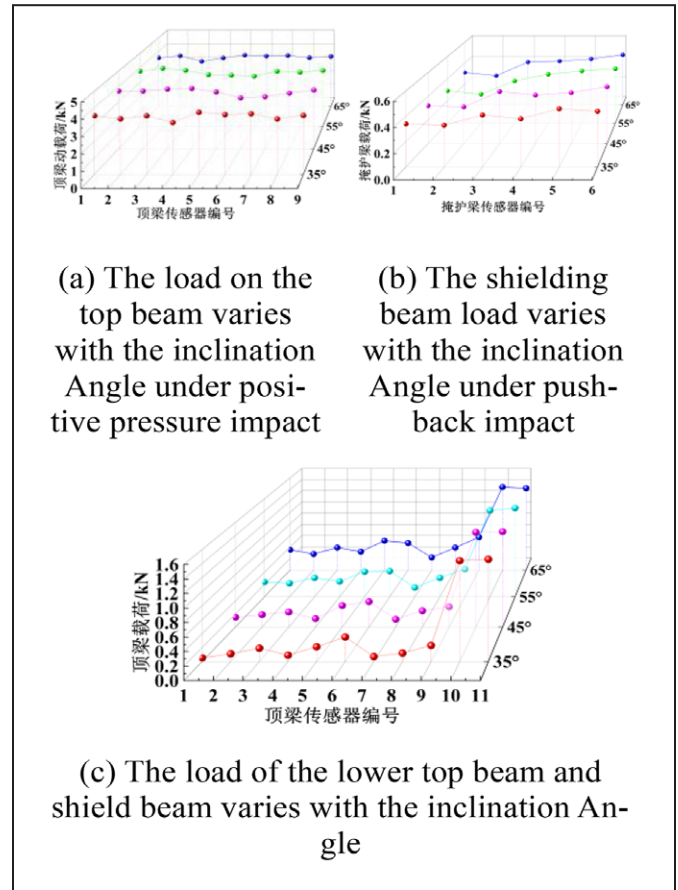


Figure 20 Changes of hydraulic support with tilt Angle under different dynamic loads

## NUMERICAL SIMULATION CALCULATION VERIFICATION

Taking two supports (interaction between analysis frames) at  $45^\circ$  inclination Angle as the research object, the dynamic load numerical simulation of hydraulic support was carried out by using FLAC 3D finite difference method under the same load environment. A 1:1 three-dimensional numerical calculation model of ZZ6500/22/48 four-column hydraulic support was established by Rhino, and the support was inclined to be arranged along the working face. As shown in Figure 21. When modeling, the top beam, shield beam, front connecting rod and back connecting rod are treated as elastomer, and the base is regarded as rigid body. The grid is divided by Rhino, and then imported into FLAC3D through Kubrix. The model contains 166,128 units and 614,201 grids.

In the hydraulic support model with large dip Angle and high mining height, the top beam, tail beam and cover beam of the support are all 16Mn steel with an elastic modulus of 208Gpa, Poisson ratio of 0.31, and density of  $7850\text{kg/m}^3$ ; the elastic modulus of the column is 980 MPa, Poisson ratio of 0.3, and density of  $7850\text{kg/m}^3$ . The power medium of the hydraulic cylinder is emulsion, and the bulk elastic modulus is 0.5GPa.

The positive impact load shown in formula (6) is applied to the top beams of the two supports at the same time to simulate the positive pressure impact. Under the positive pressure impact, the support is subjected to the strongest dynamic load, and the support is prone to instability such as compression and tipping under this type of impact. The numerical simulation results of the load on the top beam of the support group are shown in Figure 22

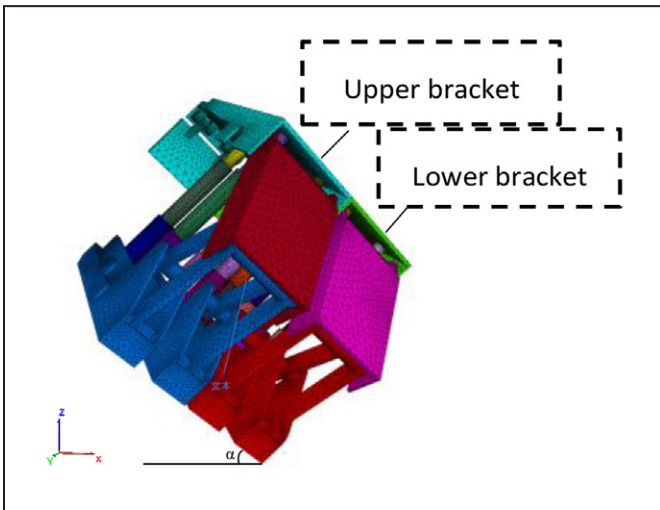


Figure 21. Numerical model diagram of support (group) for high inclination face

(a). At 20 ms, when the excitation load reaches the maximum value, it can be seen that the stress is concentrated at the side of the top beam, and the maximum stress reaches 1500 MPa. The interaction between the support frames is obvious, and even the phenomenon of biting the frame may occur. Need to do key protection. The stress of most parts of the top beam is about 250 MPa, and the stress concentration of the two supports mainly occurs at the  $2/3$  position of the top beam (that is, between the front and rear columns) during 40-60 ms, and extends to the side of the top beam. At 100 ms, the load on the top beam of the support tends to balance, the dynamic load is released, and the stress distribution of the two supports is basically symmetrical. According to the stress distribution characteristics of different time periods, it is inferred that when the top beam is impacted, the impact will be transmitted from the four columns to the base, and absorbed by the bottom plate, and the “support surrounding rock” system reaches a new balance.

For the push-back effect of the shield beam (according to Formula 6),  $P_0=383$  kN (that is, the impact effect on the support after direct push-off within the range of a single support is taken as  $27000\text{N/m}^3 \times 2.32 \text{ m} \times 1.75 \text{ m} \times 3.5 \text{ m}$ ), and the load increase amplitude  $P_r$  is taken as 60 kN to simulate the push-back impact. As shown in Figure 22 (b), tensile stress concentration occurs at  $1/3$  of the shield beam, reaching a maximum of 7 MPa, and extends from this position to both sides, showing a decreasing trend, indicating that when the shield beam is impacted, the load spreads around along the impact center, but when it is transmitted to the angular part, the dynamic load cannot be transmitted quickly and effectively, resulting in local stress concentration. The stress at the upper end of the shield beam of the two supports is greater than that at the lower end, and the stress on the lower support is greater than that on the upper support. This is because when the two supports are impacted at the same time, the upper support will be deflected and unstable, and the load will be transferred to the lower support, thus affecting the stability of the lower support. At 100 ms, except for the stress concentration at the hinged joint with the top beam, the stress of the rest parts of the shield beam is basically 0. Based on the stress distribution at different times, it can be inferred that when the shield beam is impacted, the dynamic load will spread around along the impact position, transfer to the top beam or base, and then transfer to the base and surrounding rock by the column.

For the side push load between the frames,  $P_0=615$  kN and the load increase amplitude  $P_r$  were taken to 100 kN to simulate the back push impact. As shown in Figure 22(c),

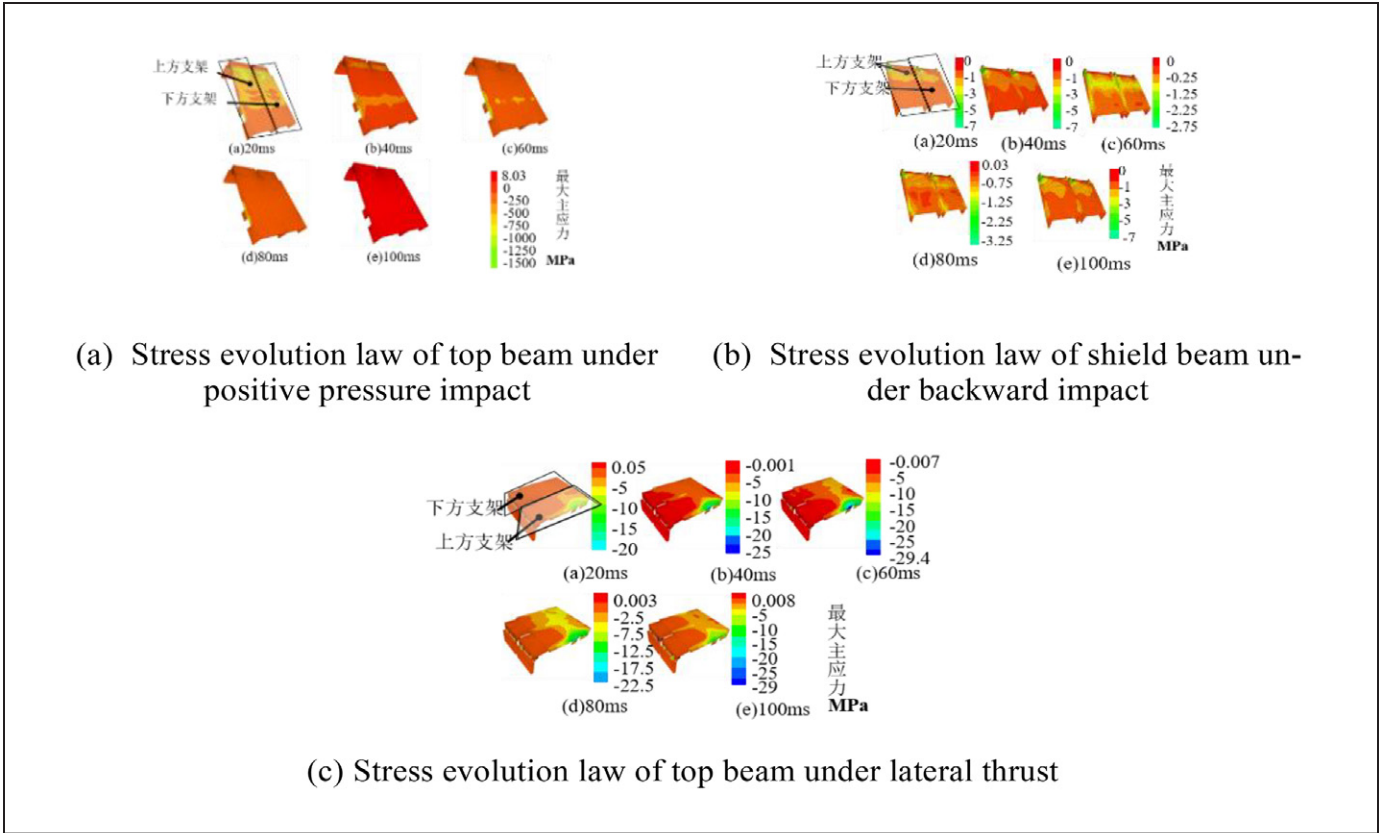


Figure 22. Stress evolution law of support under different impact

a stress concentration zone is formed at the pushing load on the applying side, with the maximum stress reaching 29 MPa. The concentration zone gradually diffuses around and gradually decreases, and the stress reaches 2.5 MPa at the contact point with the second support. The overall stress of the lower support is small, indicating that the dynamic load impact is not transmitted to the lower support at this time, and the impact on the lower support is small. At this time, the lower support is less likely to slide and lose stability. When the impact load is transmitted by the upper support at 80 ms, and the load is not balanced, the upper support is prone to toppling and losing stability. Between 80 and 100 ms, the maximum principal stress of the lower support decreases from 7.5 MPa to 2.5 MPa, so the lower support is not easy to lose stability. At 100 ms, the upper support is still affected by the side push load, and the maximum main stress at the hinged joint between the top beam and the protection plate reaches 29 MPa, which easily leads to the tipping instability of the support, and leads to the serial instability of the support group.

It can be seen that under the three kinds of impact, the load is transmitted to the four sides along the dynamic load position, and the stress concentration occurs in the position where multiple components of the hydraulic support are

hinged, and the dynamic load in this position cannot be rapidly transmitted and diffused, which is easy to cause the instability of the support. The three kinds of impact loads show asymmetric load characteristics, and the load of the lower bracket is smaller than that of the upper bracket.

The load at the bottom of all the columns is almost greater than that in the middle and upper parts. In order to reduce the impact load transfer effect of the column on the bottom plate or base, it is necessary to prevent the instability of the bracket due to the fall of the base, and the column is not easy to slide and become unstable. The above research conclusions are basically consistent with the results of physical similar simulation experiments.

Combined with the above research conclusions, the following improvement measures are proposed for the stability control of the stent:

1. Increase the contact area between the support and the bottom plate to reduce the damage probability to the bottom plate ; to prevent the subsidence of the working face support, it is usually possible to design the support base and adjust the stress state of the base by reducing the specific pressure of the

support to the floor, so as to ensure the good contact between the support and the roof and floor.

2. In the process of advancing the working face, the damage of the support to the floor due to roll is avoided. Under the condition of particularly soft floor, the ‘bottom lifting’ of the support should be considered.
3. Adding base adjustment frame and side pushing device, reinforced side guard plate, lifting base device, etc., can effectively solve the problem of support sinking under soft bottom conditions.

## CONCLUSIONS

1. The 1 : 5 large-scale laboratory hydraulic support solid model was developed. After modeling and rendering, it was imported into Unity 3D to establish an experimental-scale virtual support model, which realized the real-time sharing of the position and load data of the laboratory hydraulic support physical solid model and the twin model, and completed the development of the twin system.
2. The evolution law of support load under different inclination angles was studied by combining field measurement and physical analog experiment. That is, with the increase of the inclination Angle of the working face, first, the initial support force required by the support becomes smaller, and the damage degree of the roof increases; When the roof is soft, the lifting operation can avoid the instability of the support to a certain extent. Under static load, the load on the top beam decreases with the increase of inclination Angle. Under the effect of positive pressure, there is no obvious difference in the load of different parts of the top beam under four angles. Under the action of pushing back, the load on the upper part of the inclined shield beam is the largest, followed by the middle part, and the lower part is the smallest. With the increase of the inclination Angle, the load on the upper part of the inclined shield beam gradually increases, and the load on the lower part of the inclined shield beam gradually decreases. Under the action of lateral pushing, the load on the side of the top beam is greater than that on the surface of the top beam, and the load in each period is greater than that in the previous period.
3. Numerical simulation experiments verified the results of the above physical simulation research. In order to reduce the transmission effect of the column on the impact load of the bottom plate or

the base and avoid the instability of the support, improvement measures for the hydraulic support were proposed according to the research conclusions, and good application results were achieved.

## REFERENCES

- [1] Kulakov V.N..Stress state in the face region of a steep coal bed [J]. Journal of Mining Science, 1995(09):161168.
- [2] Bodi J. Safety and technological aspects of man less exploitation technology for steep coal seams[C].27th international conference of safety in mines research institutes,1997:955965.
- [3] Singh, T.N., Gehi, L.D.State behavior during mining of steeply dipping thick seams-A case study[C]. Proceedings of the International Symposium on Thick Seam Mining,1993: 311-315.
- [4] DREBENSTEDT C, GRAFE R. Stereoscopic 3D-display for mine planning and geological modeling, 2001[C].2001.
- [5] Daniel Gleeson. WCM’s Woodhouse Colliery met coal project heads for site work[EB/OL]. [2021-1-7].
- [6] HOLLANDS R, DENBY B, BROOKS G. SAFE-VR-A virtual reality safety training system[J]. Proceedings of APCOM’99, 1999.
- [7] Wen J R, Mu-Qing W U , Jing-Fang S U . Cyber-physical System[J]. ACTA AUTOMATICA SINICA, 2012, 38(4):507-517.
- [8] Kraft E M . The Air Force Digital Thread/Digital Twin Life Cycle Integration and Use of Computational and Experimental Knowledge[C]// 54th AIAA Aerospace Sciences Meeting, 2016.
- [9] GAMLIN A, BREEDON P, ME-DJDOUB B. Immersive Virtual Reality Deployment in a LeanManufacturing Environment[C]. International Conference on Interactive Technologies & Games.IEEE Computer Society. Nottingham, ENGLAND.2014.
- [10] Rosen R, Von Wichert G, Lo G , et al. About The Importance of Autonomy and Digital Twins for the Future of Manufacturing[J]. IF AC PapersOnLine, 2015, 48(3):567-572.
- [11] Schluse M, Rossmann J . From simulation to experimentable digital twins: Simulation-based development and operation of complex technical systems[C]// IEEE International Symposium on Systems Engineering. IEEE, 2016.
- [12] ELLGASS W, HOLT N, Saldana-Lemus H, et al. A digital twin concept for manufacturing systems[C].

- ASME International Mechanical Engineering Congress and Exposition. Pittsburgh, PA, USA. 2018.
- [13] NEGRI E, FUMAGALLI L, MAC-CHI M. A Review of the Roles of Digital Twin in CPS-Based Production Systems[J]. *Procedia Manufacturing*, 2017,11: 939-948.
- [14] KUTS V, MODONI G E, TERKAJ W, et al. Exploiting factory telemetry to support Virtual Reality simulation in robotics cell[C]. *International Conference on Augmented Reality*. Ugento, ITALY. 2017.
- [15] ZHUANG CB, LIU JH, XIONG H. Digital twin-based smart production management and control framework for the complex product assembly shop-floor[J]. *International Journal of Advanced Manufacturing Technology*, 2018,96: 1-4.
- [16] Hodgkinson J H, Elmoultie M. Cousins, Siblings and Twins: A Review of the Geological Model's Place in the Digital Mine[J]. *Resources*, 2020, 9(3):24.
- [17] Torres-Ferreyros C M, Festini-Wendorff M A, Shiguihara-Juarez P N. Developing a video-game using unreal engine based on a four stages methodology[C]// *Andescon*. IEEE, 2016. Mittring M. Finding next gen: CryEngine 2.2007.
- [18] Gestwicki Paul. Godot engine and checklist-based specifications[J]. *Journal of Computing Sciences in Colleges*, 2021.

# Explosion-Proof Enclosure Failure to Contain a Lithium-Ion Battery Thermal Runaway

Thomas H. Dubaniewicz

CDC NIOSH, Pittsburgh PA

## ABSTRACT

Gassy underground mines commonly use explosion-proof (XP) enclosures to enclose electrical ignition sources to prevent propagation of an internal methane-air explosion to a surrounding explosive atmosphere. Researchers at the National Institute for Occupational Safety and Health (NIOSH) conducted a lithium-ion battery thermal runaway test within a modified MSHA-approved XP enclosure to assess thermal runaway containment. Thermal runaway produced jet flames emanating from the cover joint at several locations and distorted the cover joint and bottom plate of the enclosure beyond allowable limits. The test demonstrates that XP enclosures may not provide adequate explosion protection against lithium-ion battery thermal runaway. This paper suggests some approaches to mitigate the hazard.

## INTRODUCTION

Lithium-ion (Li-ion) battery fires are becoming more commonplace in the United States. Fire departments across the country held a week-long safety stand-down during June 2023 themed “Lithium-Ion Batteries: Are You Ready?” [1]. Large-format Li-ion powered battery electric vehicles (BEVs) are in the early stages of deployment in underground mines in the United States. GlobalData [2] reported a total of 10 active electric Load Haul Dump (LHD) vehicles and

trucks in U.S. underground mines as of March 2022. A Li-ion BEV fire at an underground operation in Nevada prompted a U.S. Mine Safety and Health Administration (MSHA) order to suspend operations to protect the mine workers at the operation [3]. The Nevada incident represents a failure rate of well into the percent range for fires per deployed Li-ion battery LHDs and trucks in U.S. underground mines. Several Li-ion battery truck fires have occurred in Canadian underground mines as well [4, 5], representing a failure rate in the percent range for a larger sample size of 76 electric LHDs and trucks [2]. All of these incidents involved heating from short circuits external to the battery or external to multiple cells within a large battery rather than a single-cell internal short circuit.

Li-ion BEVs in gassy underground mines pose unique explosion hazards. Dubaniewicz et al. [6, 7] reviewed the gassy mine explosion hazard and the use of explosion-proof (XP) or flame-proof enclosures for explosion protection of electrical equipment. Mines commonly use XP or flame-proof enclosures in potentially explosive atmospheres to enclose electrical ignition sources to prevent propagation of an internal methane-air explosion to a surrounding methane and coal-dust-contaminated atmosphere. Emergencies involving ventilation disruption may produce explosive atmospheres. Stranded battery energy is one potential ignition hazard after mine power is shut off during such